Q. J. R. Meteorol. Soc. (1996), **122**, pp. 391–413

Vorticity asymmetries in Hurricane *Josephine* (1984)

By ARNO GLATZ and ROGER K. SMITH*
University of Munich, Germany

(Received 24 November 1994; revised 17 May 1995)

SUMMARY

A further analysis of omega dropwindsonde observations from three synoptic-flow experiments in the environment of Hurricane *Josephine* is described, complementing an earlier study by Franklin. The intensity, structure and evolution of azimuthal wave-number components of the 850–500 hPa layer-mean and deep-layer mean (surface to 100 hPa) vorticity fields, including the symmetric component, are investigated, and the determination of the extent to which the asymmetries may be interpreted in terms of the barotropic theory of vortex motion in simple large-scale environments is sought. The latter endeavour calls for a (necessarily arbitrary) partitioning of the flow between vortex and environment. As a starting point for this it is hypothesized that the environmental flow has a linear variation across a domain that appears to be encompassed by the storm circulation. Based on this assumption it is shown that, on two of the three days on which data were available, the structure and strength of the wave-number 1 vorticity asymmetry were similar to the beta-gyres that are a feature of model calculations. The day-to-day changes in the orientation and strength of these asymmetries in the 850–500 hPa layer-mean calculations are difficult to interpret in the light of barotropic theory, and are possibly associated with vertical shear in the storm environment, as described in a recent paper by Jones. Such rapid changes are not seen in the corresponding deep-layer mean calculations, but the wave-number 1 asymmetries in these fields are significantly influenced by the contributions from upper tropospheric levels where there are few data and where the vortex circulation centre is dispatched horizontally far from that at the surface.

The orientation of the wave-number 2 asymmetry varied little over the three-day observation period and was broadly consistent with the orientation of the large-scale deformation field. Moreover, its strength weakened during the period and varied monotonically with that of the deformation field, a result that is consistent also with theoretical expectations.

The attempted analysis highlights certain intrinsic problems in interpreting hurricane motion in terms of current theories. This is due partly to the non-uniqueness of the partition required to separate the storm environment from the vortex asymmetries and partly because of the difficulty of determining a representative model-equivalent value for the environmental absolute-vorticity gradient from the data.

KEYWORDS: Asymmetric flow Hurricanes Observational field experiments Tropical cyclones Vorticity

1. INTRODUCTION

Recent theoretical studies of tropical-cyclone motion in the framework of barotropic models point to the importance of large-scale asymmetries in the vorticity field in determining the cyclone motion relative to some mean current in which the vortex is embedded (Fiorino and Elsberry 1989; Shapiro and Ooyama 1990; Smith *et al.* 1990; Smith and Weber 1993; Kraus *et al.* 1995; and refs). In order to verify these theories, one must be able to extract the asymmetries from observational data reliably. Calculations by Reeder *et al.* (1991) and Weber and Smith (1995) suggest that, depending on the cyclone size, wind measurements with a horizontal resolution on the order of 100–150 km would be necessary in and around the cyclone to accomplish this extraction and, by implication, would be a necessary prerequisite to be able to initialize a storm in a forecast model accurately. At the present time, the only data sets that come close to providing such resolution are those obtained for a few Atlantic hurricanes during special field experiments organized by the Hurricane Research Division (HRD) of the NOAA†/Atlantic Oceanographic and Meteorological Laboratory. One such experiment was carried out on Hurricane *Josephine* (1984) and an analysis of the data obtained was published by Franklin (1990). This data set is unique in the sense that it remains the only one in which a storm and its environment were sampled in detail on three consecutive days.

* Corresponding author: Meteorological Institute, University of Munich, Theresienstr. 37, 80333 Munich, Germany.

† National Oceanic and Atmospheric Administration

In this paper we present additional analyses of these data with the object of investigating the vorticity asymmetries. In particular we seek to determine the scale, intensity and vertical coherence of the azimuthal wave-number 1 and 2 components of these asymmetries, and their time evolution. A further aim is to determine to what extent, if any, the structure and evolution of the asymmetries can be interpreted in terms of the behaviour of those that develop in simple-barotropic-model calculations when an initially symmetric vortex is placed in an environmental flow with uniform or linearly varying horizontal deformation and/or a uniform absolute-vorticity gradient. Such questions are relevant for two reasons: (i) because the simple-model calculations provide the basis for a conceptual understanding of vortex motion, and (ii) because these models provide a basis for constructing synthetic vortices for initializing hurricane-prediction models in situations where aircraft reconnaissance data are either unavailable or insufficient to define the initial vortex, the latter being the normal case. Finally we examine to what extent the diagnosed azimuthal wave-number 1 velocity asymmetry can account for the observed motion of Hurricane *Josephine*.

The layout of the paper is as follows. In section 2 we describe briefly the data set and the analysis methods employed. The results of the analyses are presented in section 3 and in section 4 we conclude with a discussion of outstanding problems.

2. Data and analysis

Hurricane *Josephine* was sampled on three days by two research aircraft which flew into the environment of the storm and released nearly 50 omega dropwindsondes (ODWs) during each nine-hour mission. The sondes covered an area of approximately $15^\circ \times 15^\circ$ latitude centred on the hurricane, and data between 400 hPa and 950 hPa were obtained. A description of the storm and its synoptic setting, and of the data gathered, are given by Franklin (1990).

Two objective-analysis algorithms were applied to the primary observations. The first, described by Franklin (1990), was a two-dimensional least squares fitting algorithm with a low-pass filter. The field was represented as a set of cubic splines, centred on a two-dimensional array of grid points on 19 pressure surfaces with a resolution of $1^\circ \times 1^\circ \times 50$ hPa. As the spline functions are twice-differentiable, any derived quantity can be calculated in the domain. Gridded values of the zonal and meridional wind components u and v obtained in this way and their first and second derivatives for 00 UTC on 10, 11 and 12 October 1984 were kindly provided to us by James Franklin at the HRD.

A second objective-analysis scheme was applied to the ODW data alone using a successive correction method developed by Pedder (1993). As in Franklin's analysis, the locations of the ODWs were adjusted to a storm-centred coordinate system before analysis. The u and v wind components were stored on a staggered grid and used to calculate the vorticity by line integration around each grid box. This value of the vorticity was assigned to the same location as in the HRD analysis. Some differences between the two analyses may be expected since the Pedder scheme uses only the ODW data, while the HRD analyses include data from additional sources including flight-level data from the NOAA research aircraft and USAF reconnaissance aircraft, together with rawinsonde data, ship reports, commercial aircraft pilot reports (PIREPS), and satellite-derived winds. Moreover, the HRD analyses are merged with the National Meteorological Center (NMC) wind analyses above 400 hPa.

Because there was broad agreement between the two analysis methods, the analyses shown in the following section are based on the original HRD analyses and, unless otherwise stated, relate to the pressure-weighted 850–500 hPa depth-averaged mean flow, the

layer covered by the ODW data. We show also some fields based on the deep-layer mean (DLM) flow, a pressure-weighted layer average from the surface to 100 hPa. Although in principle more suitable for comparison with barotropic-model calculations, the latter fields are influenced above the 400 hPa level to an unknown degree by the NMC assimilated analyses, which in data-sparse regions are determined largely by the NMC model prediction rather than by observational data. Another difficulty with the DLM fields is noted below.

The vortex centre of the depth-averaged flow was defined as the position of the relative-vorticity maximum and was located by a five-point interpolation using a quadratic fitting function (see, for example, Smith *et al.* 1990, appendix A). An azimuthal average was calculated about this centre and then subtracted from the total asymmetric field to give the vorticity asymmetry. Following this a Fourier analysis of the latter was carried out in the azimuthal direction to obtain the various azimuthal wave-number contributions thereto. The principal results of these analyses are described in the next section. It is worth pointing out that the centre positions calculated at individual levels differ by at most 8 km between 850 hPa and 650 hPa, and at most 15 km between 850 hPa and 500 hPa. Moreover, the centre position of the 850–500 hPa depth-averaged flow differs by 35 km from the best track position on 10 October, but by less than 18 km on the other two days. Above 300 hPa the vortex centre was ill-defined; on 10 and 11 October the relative-vorticity field had a north–south oriented dipole pattern with the cyclonic and anticyclonic centres located many hundreds of kilometres from the vortex centre at the surface. In contrast, on 12 October there were anticyclonic centres far to the north and south of the storm, with cyclonic vorticity to the west and anticyclonic vorticity to the east. These structures have a significant effect on the structure of the DLM flow asymmetries and introduce uncertainties in the interpretation of these.

3. Results

(*a*) *The environmental flow*

Despite the limited size of the domain on which ODW data were available, an attempt was made to partition the vorticity asymmetry into a 'large-scale' environmental flow component before carrying out the azimuthal averaging and the subsequent Fourier analysis. In order to facilitate the comparisons with model calculations, and also because the domain on which ODW data were obtained appeared to be comparable in scale with the scale of the cyclone circulation*, we assumed the large-scale flow to have a linear variation locally, both zonally and meridionally, across the vortex. This is equivalent to expressing the environmental flow as a double Taylor-series expansion in x and y and truncating quadratic and higher-order terms. There will always be some region over which this truncation will be accurate, and the size of this region in a particular case will depend on the degree to which the environment can be considered to be slowly varying on the radial scale of the vortex. This, in turn, will depend on the proximity of neighbouring flow features with a comparable or smaller scale to the vortex, itself. Our assumption here is that the region of tolerable accuracy extends across the analysis domain.

It is important to recognize that no partition between the vortex and its environment is unique (Kasahara and Platzman 1963) and the method chosen here may not correspond exactly to that adopted in a numerical model, a point discussed by Reeder *et al.* (1992, see section 3). Because of the non-uniqueness, one cannot determine a priori the accuracy of the foregoing approximation; rather it must be appraised in terms of the results it yields.

* See section 3(b)

The potential deficiencies of the approximation are discussed further in subsection (e) below.

We assume that, at least across the analysis domain, the zonal and meridional components of the environmental flow, $U^*(x, y)$ and $V^*(x, y)$, can be expressed as

$$U^*(x, y) = U_0 + (D_0 + E_0)x + (F_0 - \zeta_0)y \tag{1a}$$

$$V^*(x, y) = V_0 + (F_0 + \zeta_0)x + (D_0 - E_0)y \tag{1b}$$

where x and y are rectangular coordinates in the zonal (east) and meridional (north) directions, and U_0, V_0, D_0, E_0, F_0, and ζ_0 are constants giving estimates for the environmental flow across the vortex centre (U_0, V_0), the large-scale divergence (D_0), the background vorticity (ζ_0) and the large-scale stretching and shearing deformation (E_0 and F_0) respectively. If $u_{i,j}$ and $v_{i,j}$ denote the observed velocity components at the grid point (x_i, y_j), one can obtain a set of linear equations for the foregoing constants by minimizing the function

$$\Phi = \sum_i \sum_j \{(U_*(x_i, y_j) - u_{i,j})^2 + (V_*(x_i, y_j) - v_{i,j})^2\}. \tag{2}$$

These equations are obtained by setting $\partial\Phi/\partial\lambda = 0$, where λ stands for each of the unknown constants. The summation in (2) was carried out in the largest circular domain centred on the hurricane centre that could be constructed from the data available to us. This domain, which differed slightly in radius from day to day, is indicated later in Fig. 2.

The method is similar to one recently proposed by Davies–Jones (1993) for computing kinematic quantities from data at irregularly distributed observation stations. When applied to an artificial data set with a symmetric vortex imposed on a prescribed linearly varying shear flow, the method accurately recovers the deformation components E_0 and F_0, but not, of course, ζ_0 which is influenced by the presence of the vortex.

The results of the calculations are presented in subsections (d) and (e) and further aspects of the method of partitioning are discussed in appendix A, where expressions for the constants U_0, V_0, D_0, E_0, F_0, and ζ_0 are obtained in polar coordinates.

It should be noted that the part of the large-scale flow not involving ζ_0 is irrotational so that the partitioning leads to a clear separation between the environmental flow and the vorticity asymmetries, as well as the flow components associated with the latter.

(b) *Symmetric circulation*

Figure 1 shows the azimuthally averaged profiles of the 850–500 hPa layer-mean tangential velocity and relative vorticity at the three analysis times after the constant vorticity of the environment has been removed. It is evident from both fields that at radii less than 500 km, the layer-mean symmetric circulation intensified during the period that the storm was monitored. At larger radii the tangential velocity diminished slightly as the storm intensified. Note that the radius of maximum wind, about 250 km, is relatively large, a reflection of the inability of the data to resolve the inner core region of the storm rather than reality (see Franklin 1991 p. 2734). Especially noteworthy is the fact that, on each day, the relative vorticity was negative beyond a certain radius r_* which ranged between 400 and 450 km. This implies a decay of the mean tangential velocity with radius that is faster than $1/r$ for $r > r_*$. Significantly, estimates for the large-scale vorticity ζ_0, presented in section (d), are more than an order of magnitude smaller than the vorticity values at outer radii in Fig. 1.

Note that the radius at which the symmetric vorticity changes sign defines a radial scale for the vortex circulation. In the present case, this radius corresponds approximately

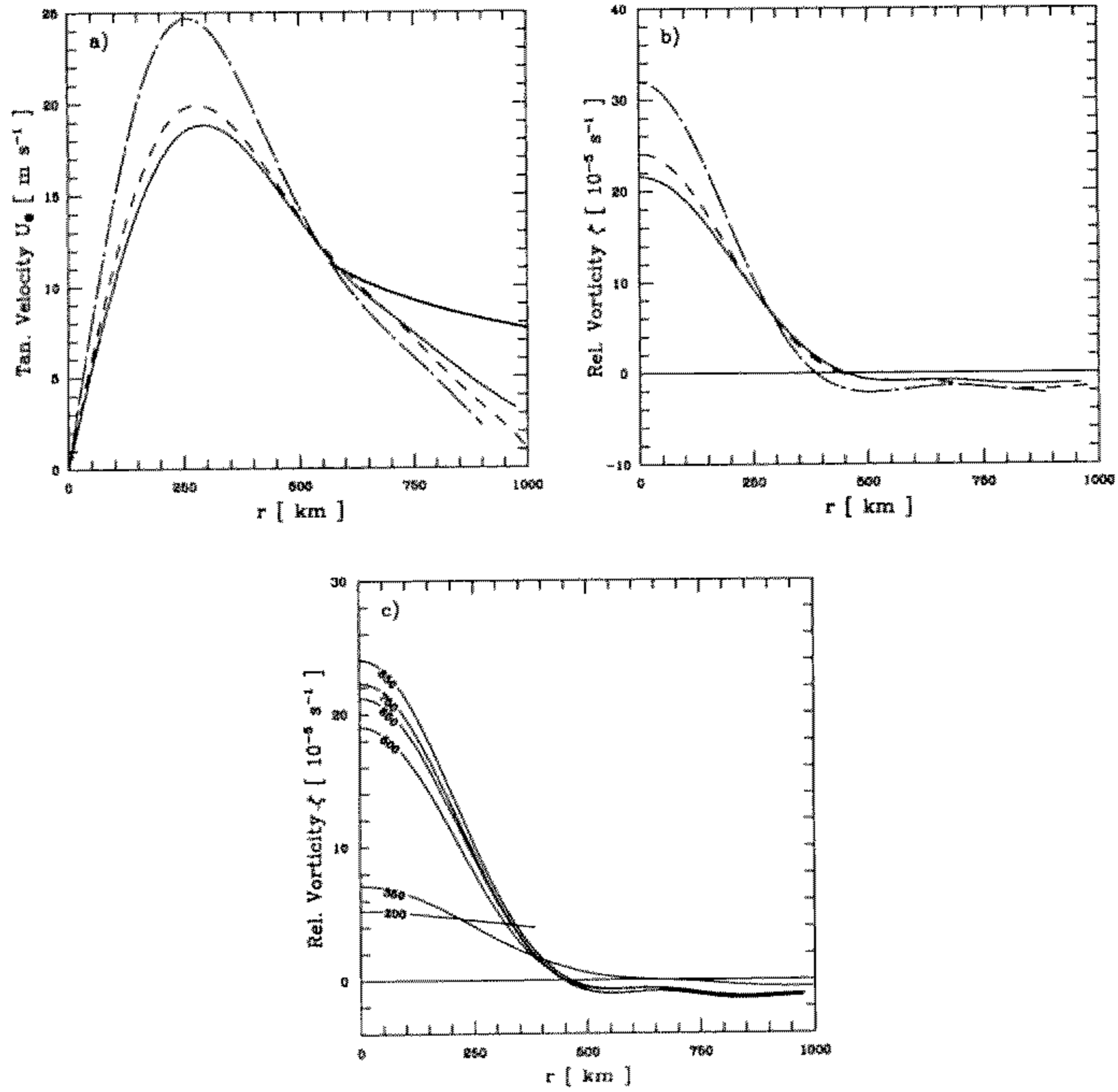

Figure 1. Radial profiles of (a) symmetric tangential velocity and (b) relative vorticity on the three analysis days 10, 11 and 12 October 1984 for the 850–500 hPa layer-mean flow. Solid lines for 10 October, short dashed lines for 11 October, dash-dot lines for 12 October. The thick solid line shows a profile in which the tangential velocity decays inversely with radius. Panel (c) shows the symmetric relative-vorticity profiles at selected pressure levels (values in hPa indicated on curves) on 10 October.

with the radius to which gale-force winds occur. However, mean tangential wind speeds exceeding 5 m s^{-1} extended to over 800 km from the vortex centre.

Shown also in Fig. 1 are the azimuthally averaged relative-vorticity profiles on different isobaric surfaces between 850 hPa and 200 hPa on 10 October. The profiles are broadly similar between 850 hPa and 500 hPa, but show a gradual decrease in the central maximum with height. At these levels the radius of zero vorticity is the same. Above 500 hPa the profiles broaden and weaken, but this may be as much a reflection of the paucity of data at these heights than of reality. The variation of the symmetric vorticity with height at the other analysis times was similar.

(c) *Azimuthal wave-number 1 asymmetry*

The azimuthal wave-number 1 contribution ζ_a to the 850–500 hPa layer-mean relative-vorticity asymmetry is shown in Fig. 2 at each analysis time, together with the wave-number

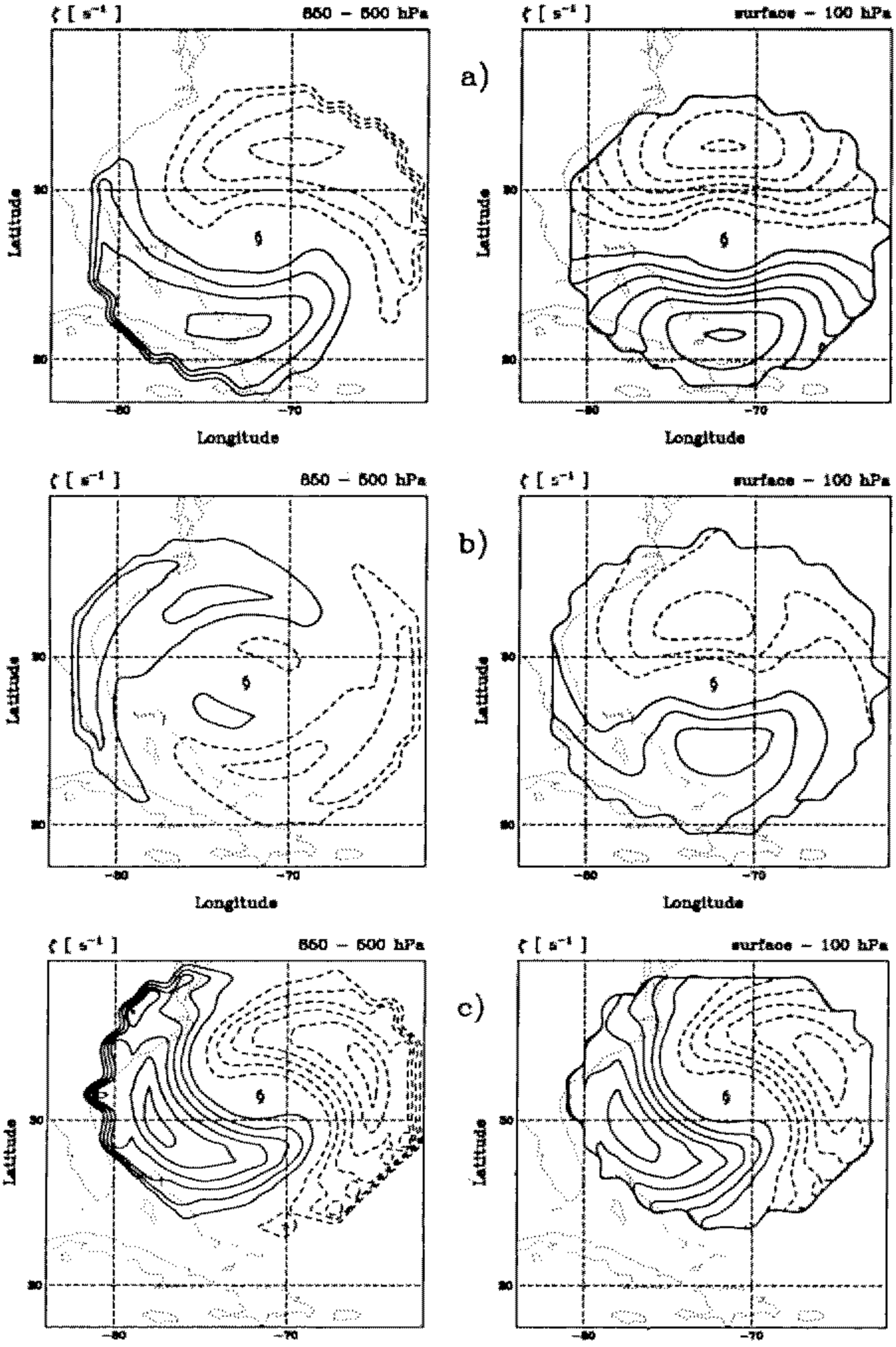

Figure 2. Wave-number 1 relative-vorticity asymmetries of the 850–500 hPa layer-mean flow (left panels) and deep-layer mean flow (right panels) on (a) 10 October, (b) 11 October, and (c) 12 October 1984. Contour interval 2.5×10^{-6} s^{-1} and dashed lines indicate negative values.

1 contribution to the DLM vorticity. We consider first the 850–500 hPa layer-means. On 10 and 12 October 1984 the wave-number 1 asymmetry was remarkably similar in scale, structure and strength to that which arises in the prototype problem in the theory of tropical-cyclone motion (see, for example, Smith *et al.* 1990, Fig. 3), the problem that considers the subsequent motion of an initially symmetric vortex on a beta-plane when there is zero basic flow. However, there were major changes in the orientation of the gyres during the period over which the storm was monitored. In particular, the axis joining the maxima and minima of the gyres (the outer gyres on 11 October) retrogressed some 90° between 10 October and 11 October, but had largely returned to its previous orientation by 12 October. Bearing in mind the mechanism for the establishment of the gyres in the foregoing prototype problem (see, for example, Smith and Ulrich 1993, section 3), it is difficult to explain such rapid changes on the basis of the simple barotropic models. One possibility is that the data gap to the north-west of *Josephine* on 10 October, caused by a failure of the ODW system on one of the aircraft, has led to an inaccurate analysis of the asymmetries on this day. However, it is appropriate to consider alternative explanations.

A limitation of the simple theories is the assumption that any changes in the large-scale vortex environment are slowly varying in time and on the spatial scale of the vortex, but they do indicate a significant time (on the order of a day) for the vortex to adjust to a specific environment (see, for example, Smith and Ulrich (1993)). Unfortunately it is difficult to quantify such changes in the time period of the present observations although Franklin (1990) notes that the ridge to the north-west of the storm weakened significantly as a mid-latitude short wave edged into the domain by 12 October. What would be required is to determine changes in the absolute-vorticity gradient of the vortex environment, but this raises difficulties which we discuss below. Nevertheless, it seems to us implausible that the changes would be large enough to account for the rapid observed changes in the wave-number 1 asymmetry. One possibility is that these changes were a reflection of baroclinic effects, i.e. a manifestation of vertical shear. As shown in a recent paper by Jones (1995), the presence of vertical shear acting on an initially symmetric vortex on an f-plane leads to a wave-number 1 asymmetry in the vorticity field that rotates on a time-scale of a day. This interpretation would be consistent also with the observation by Franklin 1990 (p. 2736) that 'the environmental flow for Hurricane *Josephine* had a strong directional shear with low-level easterlies veering nearly 180° by 500 hPa'. It is difficult to make a proper assessment of this possibility because Jones's calculations pertain to a dry vortex. In reality, the asymmetric patterns of low-level convergence that arise in these calculations would be expected to be favoured areas for deep convection, the development of which would influence the vorticity patterns also. The patterns of asymmetric convergence and divergence calculated for the 3 days of *Josephine* show a considerable day-to-day variability and are difficult to relate to the calculated vorticity asymmetries.

Another interpretation of the foregoing results would be that the method of extracting the 'large-scale environment' used here is inappropriate and that the observed asymmetries are not forced by the interaction between the storm circulation and its environment, but that they are integral features of the environment, itself. We investigate this possibility in subsection (e) below.

Finally, it might be argued that the barotropic theory applies only to the DLM flow for which the divergence should be relatively small. In this regard it is interesting to note that there is *not* a major change in the orientation of the DLM wave-number 1 asymmetries between 10 and 11 October, a fact that would tend to support the hypothesis that baroclinic effects were important in determining the structure of the 850–500 hPa layer-mean wave-number 1 asymmetry. However, there is still a marked retrogression of the asymmetries

between 11 and 12 October which is difficult to explain on the basis of barotropic theory. Note that the differences between the structures and orientation of the 850–500 hPa layer-mean and the DLM asymmetries are much less on 10 and 12 October, although the DLM fields are fractionally stronger. Unfortunately, it remains uncertain whether the contributions to the DLM flow can be considered at all realistic for the reasons discussed in section 2.

We show below that the changes in the 850–500 hPa layer-mean wave-number 2 asymmetry during the same period of observations were far less dramatic than for wave-number 1.

Since the foregoing vorticity asymmetries are for a layer mean, it is important to enquire about their structure at individual levels. The variation in structure with height up to a 500 hPa, approximately the layer for which ODW data were available, is shown in Fig. 3 for 10 October 1984. In broad terms there is good vertical consistency in both the gyre structure and strength between 850 and 650 hPa, but the 500 hPa gyre pattern is notably different in orientation from that at lower levels. Similar results were obtained on the other two analysis days. In particular, the retrogression of the gyres between 10 October and 11 October was present at all levels between 850 hPa and 600 hPa, as was the return in orientation between 11 October and 12 October.

Figure 3 shows also the corresponding gyre structures at 500 hPa and 750 hPa obtained using the Pedder analysis scheme. These fields are a little smoother than in the HRD analyses and the gyre magnitudes are slightly stronger at both levels. Significantly, the gyre axes are rotated clockwise with respect to their HRD counterparts, by 20 at 750 hPa and 45 at 500 hPa. Presumably, the large discrepancy at 500 hPa is due to the inclusion in the HRD analyses of additional data (see section 2).

(*d*) *Azimuthal wave-number 2 asymmetry*

Figure 4 shows the 850–500 hPa layer-mean wave-number 2 asymmetry at the three analysis times. It is noteworthy that the orientation of the asymmetry remained rather uniform, but its strength weakened during the 48 h period. Both the scale and strength of the asymmetry are similar, the latter within a factor 2–3, to that which occurred in the calculation by Smith (1991, see Fig. 1) for a tropical-cyclone-scale vortex in a uniform zonal shear flow of magnitude 5 m s^{-1} per 1000 km, but the orientation is manifestly different. It is natural to enquire whether the observed wave-number 2 asymmetry can be accounted for by the theory which we review briefly below.

In the analytic theory worked out by Smith (1991), it was shown that the principal contribution to the wave-number 2 asymmetry arises from the presence of large-scale deformation, and that the orientation of the asymmetry is related to that of the axis of dilatation of the deformation field. This contribution arises from the differential advection of symmetric vorticity by the large-scale flow $\mathbf{U}$ which produces asymmetric vorticity at the rate $-\mathbf{U} \cdot \nabla \zeta_v$ where ζ_v denotes the symmetric vortex vorticity. Typically, the largest contribution to this rate of production is

$$-\tfrac{1}{2} r (\mathrm{d}\zeta_v/\mathrm{d}r)(E_0 \cos 2\theta - F_0 \sin 2\theta)$$

where (r, θ) denote polar coordinates located at the vortex centre with $\theta = 0$ pointing eastwards and E_0 and F_0 are as defined in subsection (a)—see Smith (1991, Eq. 4.14). This expression may be written in terms of the total deformation $E' = \sqrt{(E_0^2 + F_0^2)}$, whose dilatation axis is oriented at an angle $\Lambda = \frac{1}{2} \tan^{-1}(F_0/E_0)$ measured counterclockwise from east, i.e.

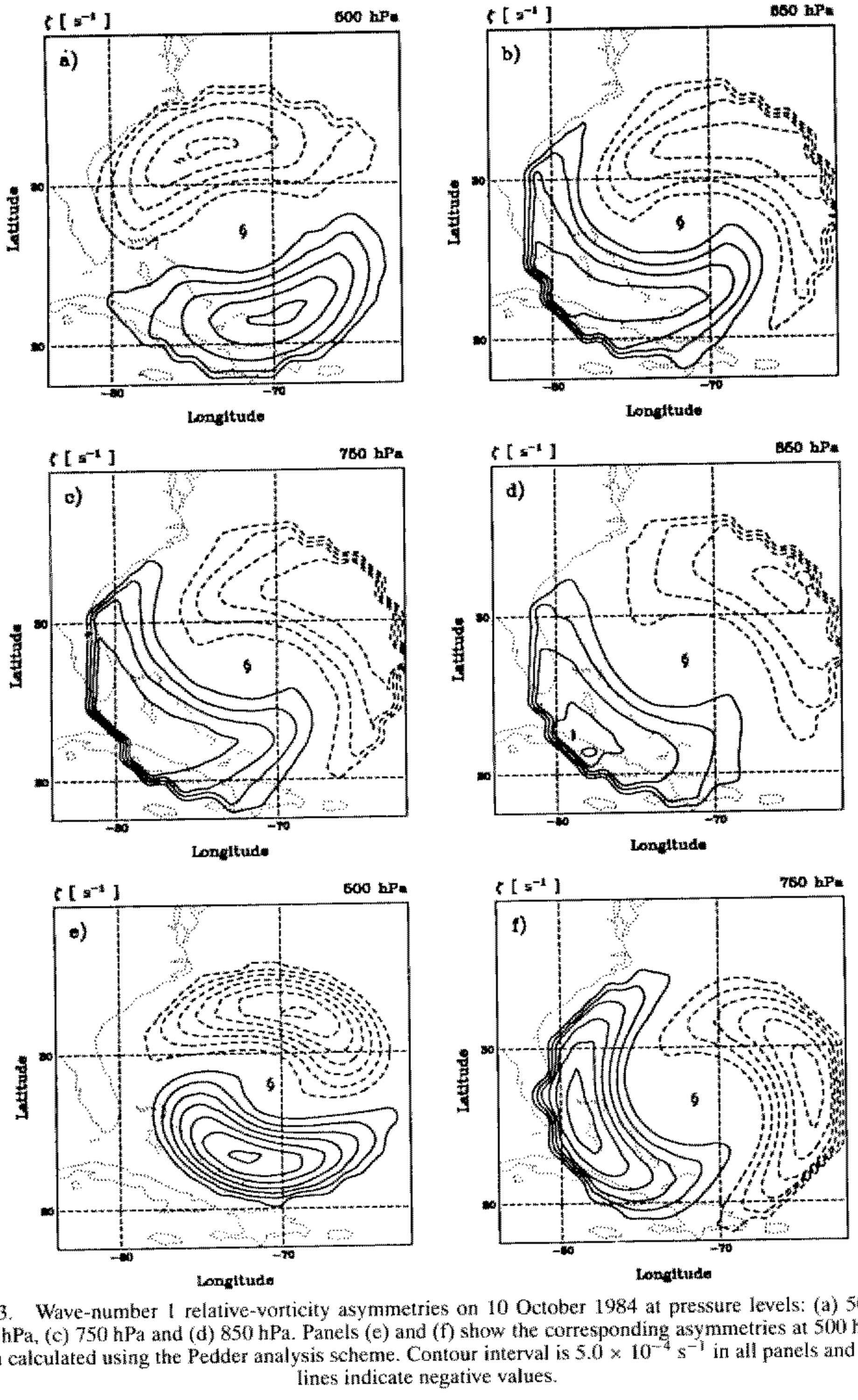

Figure 3. Wave-number 1 relative-vorticity asymmetries on 10 October 1984 at pressure levels: (a) 500 hPa, (b) 650 hPa, (c) 750 hPa and (d) 850 hPa. Panels (e) and (f) show the corresponding asymmetries at 500 hPa and 750 hPa calculated using the Pedder analysis scheme. Contour interval is 5.0×10^{-4} s^{-1} in all panels and dashed lines indicate negative values.

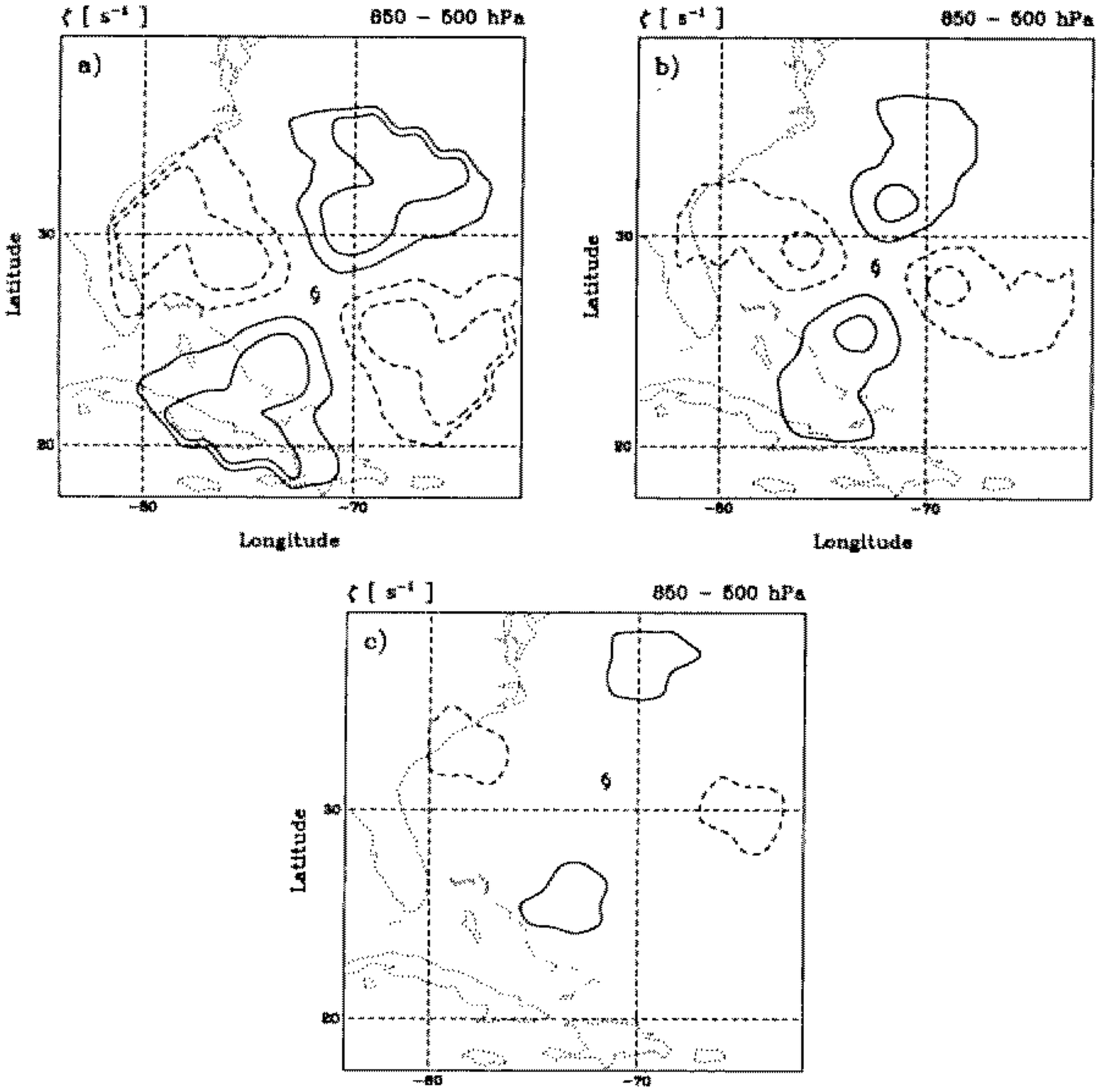

Figure 4. Wave-number 2 relative-vorticity asymmetries of the 850–500 hPa layer-mean flow on (a) 10 October, (b) 11 October, and (c) 12 October 1984. Contour interval is 5.0×10^{-6} s^{-1} in all panels and dashed lines indicate negative values.

$$\tfrac{1}{2}r(\mathrm{d}\zeta_v/\mathrm{d}r)E' \cos\{2(\theta - \Lambda)\}.$$

This corresponds with a wave-number 2 asymmetry in the vorticity tendency directed along the axis of dilatation of the local deformation. Accordingly the wave-number 2 asymmetry, ζ_{a2}, satisfies the equation

$$\frac{\partial \zeta_{a2}}{\partial t} + \Omega(r, t)\frac{\partial \zeta_{a2}}{\partial \theta} = \frac{1}{2}r(\mathrm{d}\zeta_v/\mathrm{d}r)E' \cos\{2(\theta - \Lambda)\} \tag{3}$$

where $\Omega(r, t)$ is the angular velocity at radius r at time t.

In the case of a zonal shear flow $\mathbf{U} = (U(y), 0)$, $E_0 = 0$ and $F_0 = -\mathrm{d}U/\mathrm{d}y$, whereupon $\theta = 45^\circ$ and if F_0 is nonzero one obtains the pattern shown schematically by Smith (1991, Fig. 5(c)). The actual asymmetric vorticity associated with such a pattern is slightly rotated clockwise because of advection by the symmetric vortex circulation—see, for example, Smith (1991, Fig. 6(a)). In general, of course, the large-scale shear will not be zonal, and calculations for a more complicated basic state have been carried out by Kraus *et al.* (1995).

TABLE 1. VALUES OF THE CONSTANTS U_0 AND V_0 IN EQ. (1) FOR THE THREE ANALYSIS TIMES. THE FIRST TWO COLUMNS OF U_0 AND V_0 GIVE THE VALUES CALCULATED FROM THE TOTAL WIND DATA, THE SECOND TWO COLUMNS ARE BASED ON WIND DATA WITH THE SYMMETRIC VORTEX REMOVED

Date	Total fields		Vortex removed	
	U_0 (m s^{-1})	V_0 (m s^{-1})	U_0 (m s^{-1})	V_0 (m s^{-1})
10 October 1984	−2.4	1.5	−2.4	1.6
11 October 1984	1.1	1.6	1.1	1.5
12 October 1984	−0.0	2.7	0.2	2.8

TABLE 2. AS FOR TABLE 1, BUT FOR THE RELATIVE VORTICITY, ζ_0, AND DIVERGENCE, D_0

Date	Total fields		Vortex removed	
	ζ_0 (s^{-1})	D_0 (s^{-1})	ζ_0 (s^{-1})	D_0 (s^{-1})
10 October 1984	2.2×10^{-5}	-1.6×10^{-6}	1.7×10^{-8}	-1.6×10^{-6}
11 October 1984	1.8×10^{-5}	-8.9×10^{-7}	6.0×10^{-8}	-8.9×10^{-7}
12 October 1984	2.7×10^{-5}	-1.0×10^{-6}	-1.5×10^{-7}	-1.0×10^{-6}

TABLE 3. AS FOR TABLE 1, BUT FOR THE STRETCHING DEFORMATION, E_0, AND SHEARING DEFORMATION, F_0

Date	Total fields		Vortex removed	
	E_0 (s^{-1})	F_0 (s^{-1})	E_0 (s^{-1})	F_0 (s^{-1})
10 October 1984	8.4×10^{-6}	3.2×10^{-6}	8.1×10^{-6}	3.0×10^{-6}
11 October 1984	5.5×10^{-6}	4.9×10^{-6}	5.5×10^{-6}	4.6×10^{-6}
12 October 1984	6.5×10^{-6}	4.4×10^{-8}	6.7×10^{-6}	-2.7×10^{-7}

TABLE 4. AS FOR TABLE 1, BUT FOR THE TOTAL DEFORMATION, E', AND THE ANGLE Λ MADE BY THE AXIS OF DILATATION WITH THE x (EAST) AXIS. THE LAST COLUMN LISTS THE ORIENTATION OF THE WAVE-NUMBER 2 ASYMMETRY, η. THE ANGLES Λ AND η ARE MEASURED ANTICLOCKWISE FROM EAST IN DEGREES

Date	Total fields		Vortex removed		
	E' (s^{-1})	Λ	E' (s^{-1})	Λ	η
10 October 1984	9.0×10^{-6}	11	8.6×10^{-6}	10	62
11 October 1984	7.4×10^{-6}	21	7.2×10^{-6}	20	73
12 October 1984	6.5×10^{-6}	0	6.7×10^{-6}	−1	75

In order to relate the observed wave-number 2 patterns to the theory, one must be able to extract the large deformation across the vortex centre from the data. This is accomplished by choosing the linear variation for the large-scale flow given by Eq. (1).

We consider first the observations. The results of the analysis described in subsection (a) when applied to the gridded data for Hurricane *Josephine* are summarized in Tables 1–4. As expected, there are some differences in the estimates for the various constants, depending on whether or not the symmetric vortex is removed from the data before

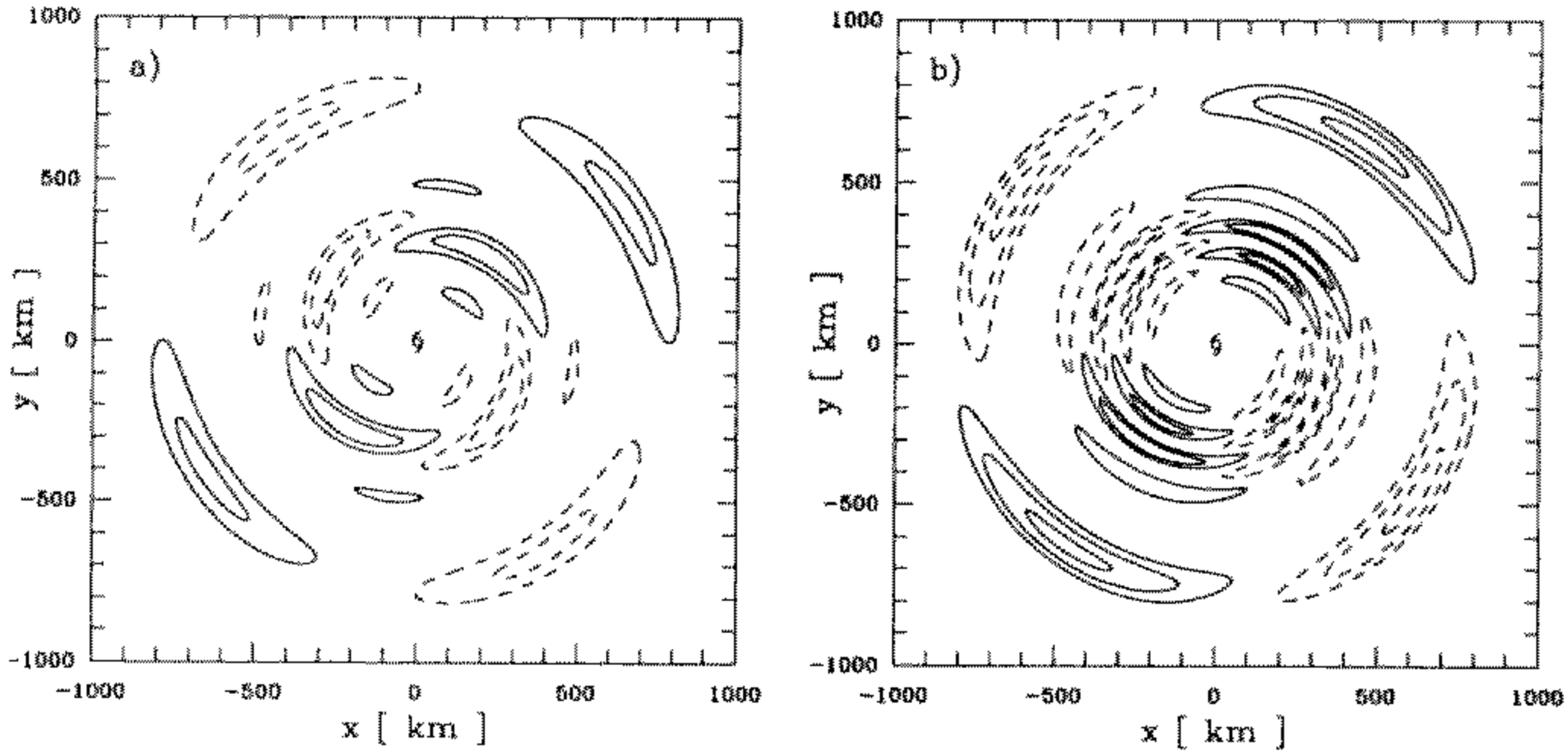

Figure 5. Wave-number 2 vorticity asymmetry produced by a uniform large-scale deformation field with the strength and orientation of that observed in Hurricane *Josephine* on 10 October 1984, acting on the observed symmetric circulation on that day: (a) after 24 hours and (b) after 48 hours. The contour interval is 5.0×10^{-4} s^{-1} and dashed lines indicate negative values.

applying the algorithm. However the total deformation (E') and the orientation of the deformation field (Λ) are almost insensitive to the presence or absence of the symmetric vortex. The axis of contraction of the deformation field changed relatively little, no more than 21°, during the three days of measurements. This is consistent with the small change in the orientation of the wave-number 2 asymmetry which is listed in Table 4 also. Furthermore, the asymmetry is rotated clockwise with respect to the axis of contraction of the deformation field in line with expectations from the analytic theory. The amount of rotation is 51° on 10 October and 51° on 11 October, but increases to 76° on 12 October.

It is difficult to compare these directly with model results as the latter vary with time also. However, it is instructive to enquire what wave-number 2 asymmetries would be produced by the flow deformation present in Hurricane *Josephine's* immediate environment acting on the observed symmetric vorticity profile of the storm on the time-scale of a day or two. The results of such a calculation using the observed symmetric vorticity profile and analysed deformation on 10 October are shown in Fig. 5. Features to note are:

• After 24 hours (Fig. 5(a)) the magnitude of the asymmetry is comparable with the observed magnitude and, like the observed field (Fig. 4(a)), there are two significant radial maxima. These occur at radii of 330 km and 760 km from the vortex centre. Moreover, the orientation is very similar to that observed and varies only slowly with time. Presumably, the dropwindsonde data would not be adequate to resolve the narrow radial scale of the calculated features so that, at best, those observed would appear like a smoothed out version of those calculated.

• After 48 hours the asymmetry at outer radii has rotated cyclonically by about 20° and strengthened a little, while at inner radii the orientation has barely changed. At first sight this may seem surprising, because the angular velocity of the symmetric circulation at radii inside 450 km is more than 160° per day compared with 32° per day at 850 km. However, one must bear in mind that the maximum asymmetric vorticity is not simply advected: wave-number 2 vorticity is continually being generated *in situ* because of the deformation-induced source term on the right-hand side of Eq. (3). Clearly the vorticity field has suffered

a marked filamentation by the radial shear of the tangential wind, represented by the second term on the left-hand side of Eq. (3).

• When the deformation rate and vortex profile do not vary with time, the strength of the asymmetry increases slowly. In contrast, the amplitude of the observed wave-number 2 asymmetry decreased with time. This could be attributable to the decrease in the observed strength of the deformation rate with time, coupled with the filamentation referred to above which moves the asymmetry to unresolved scales.

(e) *The partitioning problem*

One might question the partitioning we have used and argue that both the observed wave-number 1 and 2 asymmetries are a reflection of the neighbouring synoptic systems which included ridges to the north-west and south-east of the storm and the remains of a frontal trough extending south-west to north-east of it. We shall show that the extent to which this may be so is related to the extent to which such systems are intrinsically baroclinic. To begin with, let us assume that barotropic dynamics are applicable. If this were the case, we would argue that within the observational domain, the analysed patterns could not survive the strong tangential shear of the symmetric circulation of the hurricane during the 48-hour observation period, but would suffer major distortion. Moreover, they would undergo appreciable rotation by the storm circulation. The amount of rotation and distortion that would occur by these processes may be estimated as follows. If the wave-number 1 vorticity at time $t = 0$ is

$$\zeta_{a1} = \zeta_1(r)\cos(\theta - \alpha) \tag{4}$$

the distribution at time t would satisfy the equation

$$\frac{\partial \zeta_{a1}}{\partial t} + \Omega(r, t)\frac{\partial \zeta_{a1}}{\partial \theta} = 0. \tag{5}$$

The characteristic surfaces of this equation satisfy $\partial\theta/\partial t = \Omega(r, t)$, and ζ_{a1} is constant along such surfaces in (r, θ, t) space. If we approximate $\Omega(r, t)$ by the linear relationship $\Omega(r, 0) + d\Omega(r)t$, where $d\Omega(r)$ is the rate-of-change of $\Omega(r, t)$ with respect to time during the time interval of interest, then the characteristic surfaces have the form $\theta = \theta_0 + \Omega(r)t + \frac{1}{2}d\Omega(r)t^2$, where θ_0 is the initial value of θ at radius r. A similar calculation would apply to the wave-number 2 asymmetry by solving Eq. (3) with zero right-hand side.

Figure 6(a) shows the effect that the tangential circulation of Hurricane *Josephine* would have after 24 hours if acting alone on the analysed wave-number 1 vorticity asymmetry on 10 October. The pattern bears little resemblance to that observed (see Fig. 2(b)) and indicates that a significant counter-clockwise rotation of the asymmetry would be expected, even at radii beyond 500 km from the storm centre. There is pronounced filamentation of the asymmetry at smaller radii which would not be resolved by the ODW observations, even if it occurred in nature. Figure 6(b) shows the analogous calculation starting with the analysis on 11 October. In this case, the orientation of the asymmetry corresponds well with that observed, but the observed magnitude is significantly larger. With the assumption that the motion is barotropic we would be led to infer that the asymmetries are being forced and that they are certainly not pre-storm environmental debris. Moreover, because they occur where the tangential circulation is appreciable, one may surmise that they are linked to an interaction between the vortex circulation and its immediate environment.

In a simple barotropic model where the environment has a uniform absolute-vorticity gradient $B(\cos\chi, \sin\chi)$, the principal forcing term on the right-hand side of Eq. (5)

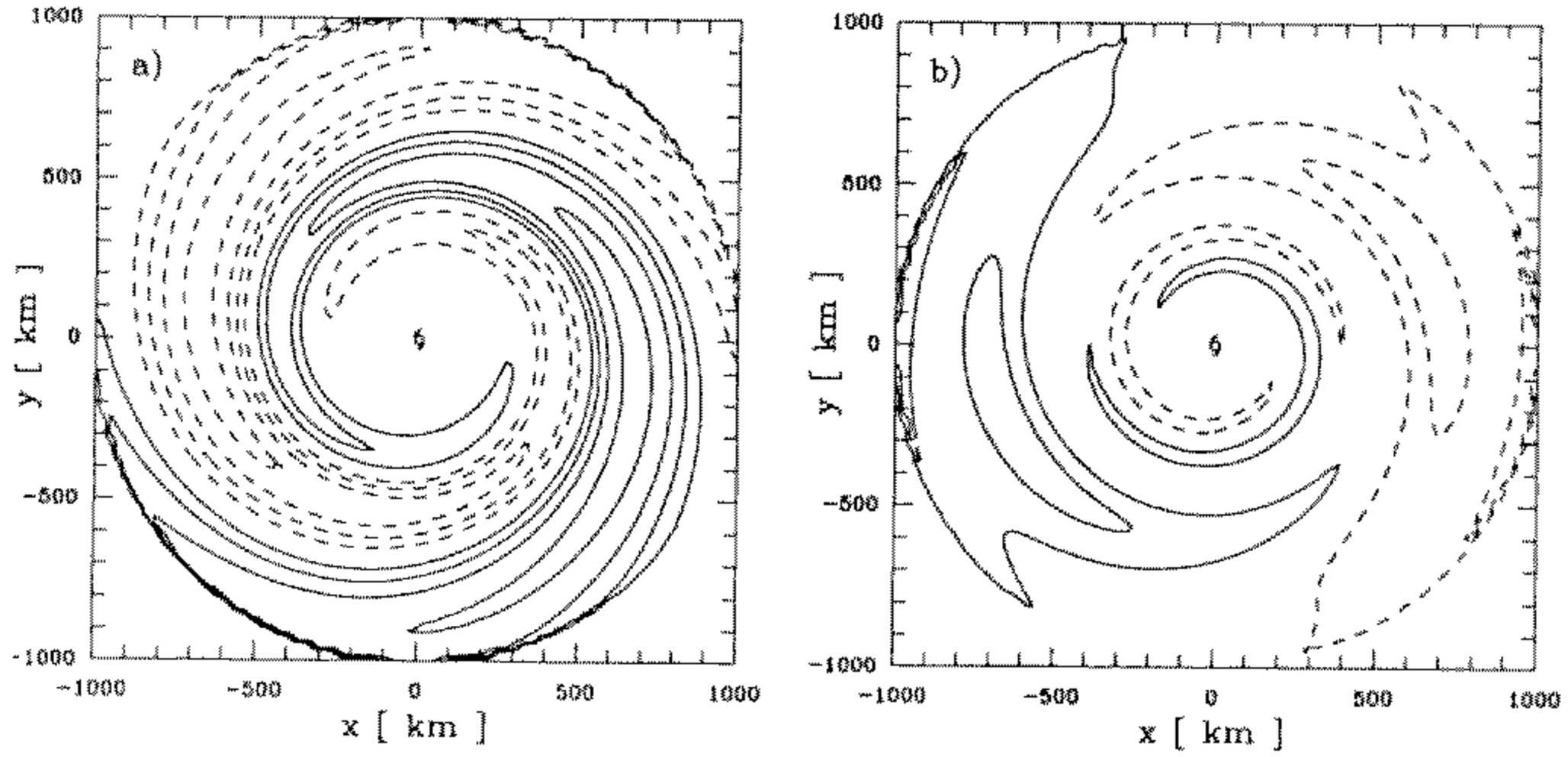

Figure 6. Hypothetical wave-number 1 relative-vorticity asymmetries of the 850–500 hPa layer-mean flow on (a) 11 October and (b) 12 October, calculated on the assumption that the observed asymmetries on 10 October and 11 October, respectively, are simply advected by the mean tangential circulation during the relevant 24-hour period. These two panels should be compared with the observed asymmetries shown in the left panels of Figs. 2(b) and 2(c), respectively.

would be $-Bv(r, t)\sin(\theta - \chi)$, where $v(r, t)$ is the tangential velocity of the symmetric circulation. Then the solution of this equation would give a leading approximation to the model beta-gyres. Unfortunately, there appears to be a fundamental difficulty in extracting an appropriate model-equivalent to the absolute-vorticity gradient from the data. Any sound procedure devised to do this would need to be applicable to the model-generated zero-order absolute-vorticity asymmetry in the case of a vortex drifting in an environment with zero basic flow where $B = \beta$ and $\chi = 0$. The pattern of absolute-vorticity gradient after 48 hours of model time in this case is shown in Fig. 7(a). Note that values are large locally compared with the planetary vorticity gradient; moreover, the annular average of the absolute-vorticity-gradient vector, which in this case can be calculated analytically, is not zero. Indeed, as indicated in Fig. 7(b), this average is sensitive to the particular annulus chosen, and it differs significantly from the prescribed environmental value $(\beta, 0)$ in the model, both in magnitude and direction. It follows that it is not possible to estimate the degree of the barotropic forcing of the wave-number 1 vorticity asymmetry, as was done for wave-number 2.

The calculations corresponding to Figs. 6(a) and 6(b), but for the wave-number 2 asymmetries are shown in Fig. 8. Again, to the extent that these are governed by barotropic dynamics, they would suffer significant rotation and filamentation as indicated in the figures (compare Figs. 8(a) and 8(b) with Figs. 4(b) and 4(c), respectively). Thus, unless the asymmetries are dominated by baroclinic effects (see below), the assumption that the analysed wave-number 2 patterns are fossil remains of systems in the pre-storm environment cannot be supported.

(*f*) *Baroclinic effects*

It is reasonable to expect that an extension of the simple barotropic ideas of vortex motion to vortex flows which are intrinsically baroclinic can be obtained by an investigation of potential-vorticity structures as opposed to relative-vorticity structures, since in adiabatic, frictionless motion, it is the Ertel potential vorticity (PV) rather than absolute

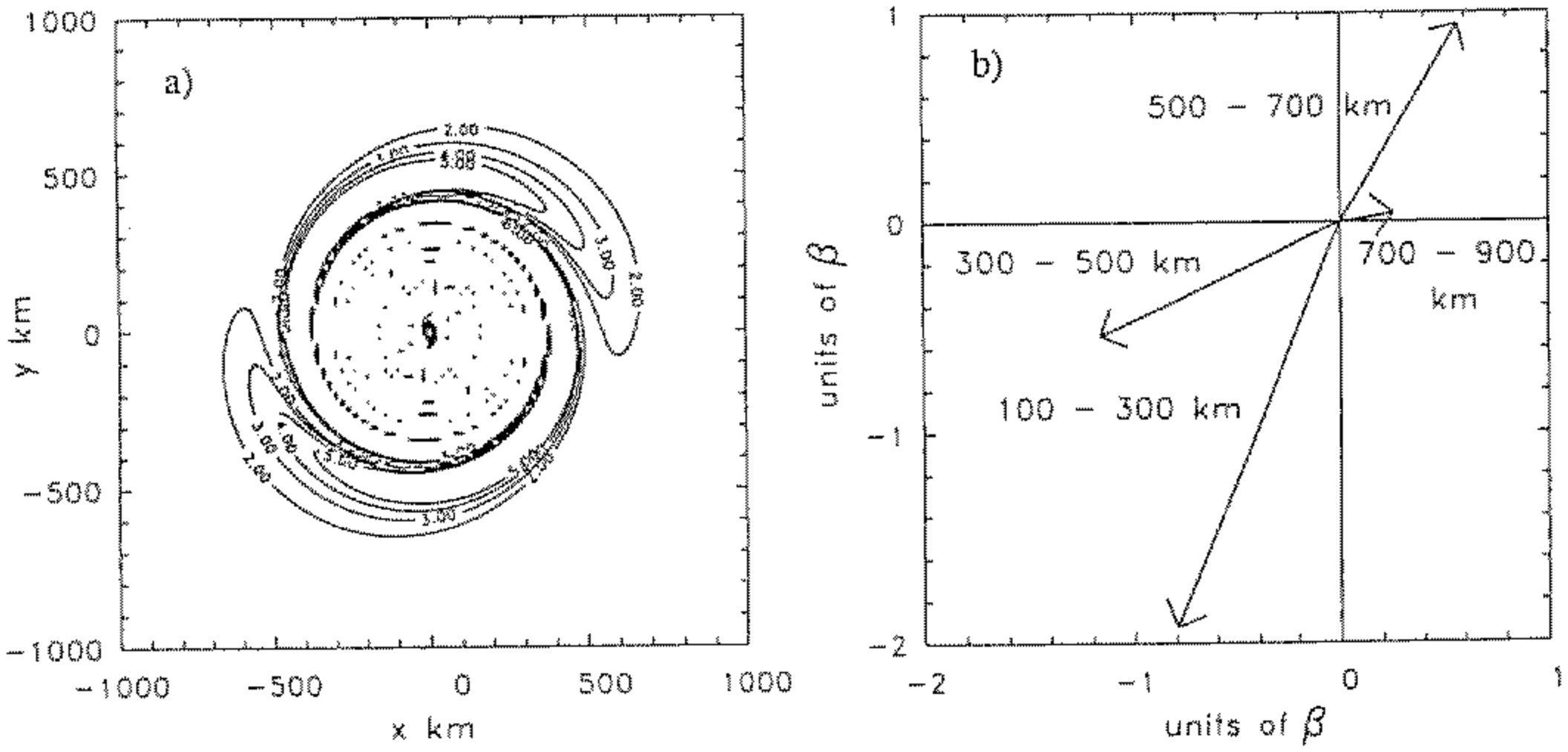

Figure 7. (a) Contours of the absolute-vorticity-gradient magnitude for an initially symmetric barotropic vortex moving on a beta-plane in the absence of an environmental flow after 48 hours, based on the zero-order solution given by Smith and Ulrich (1990). Contour levels are in units of beta. (b) Vectors representing selected annular averages of the absolute-vorticity gradient corresponding with (a).

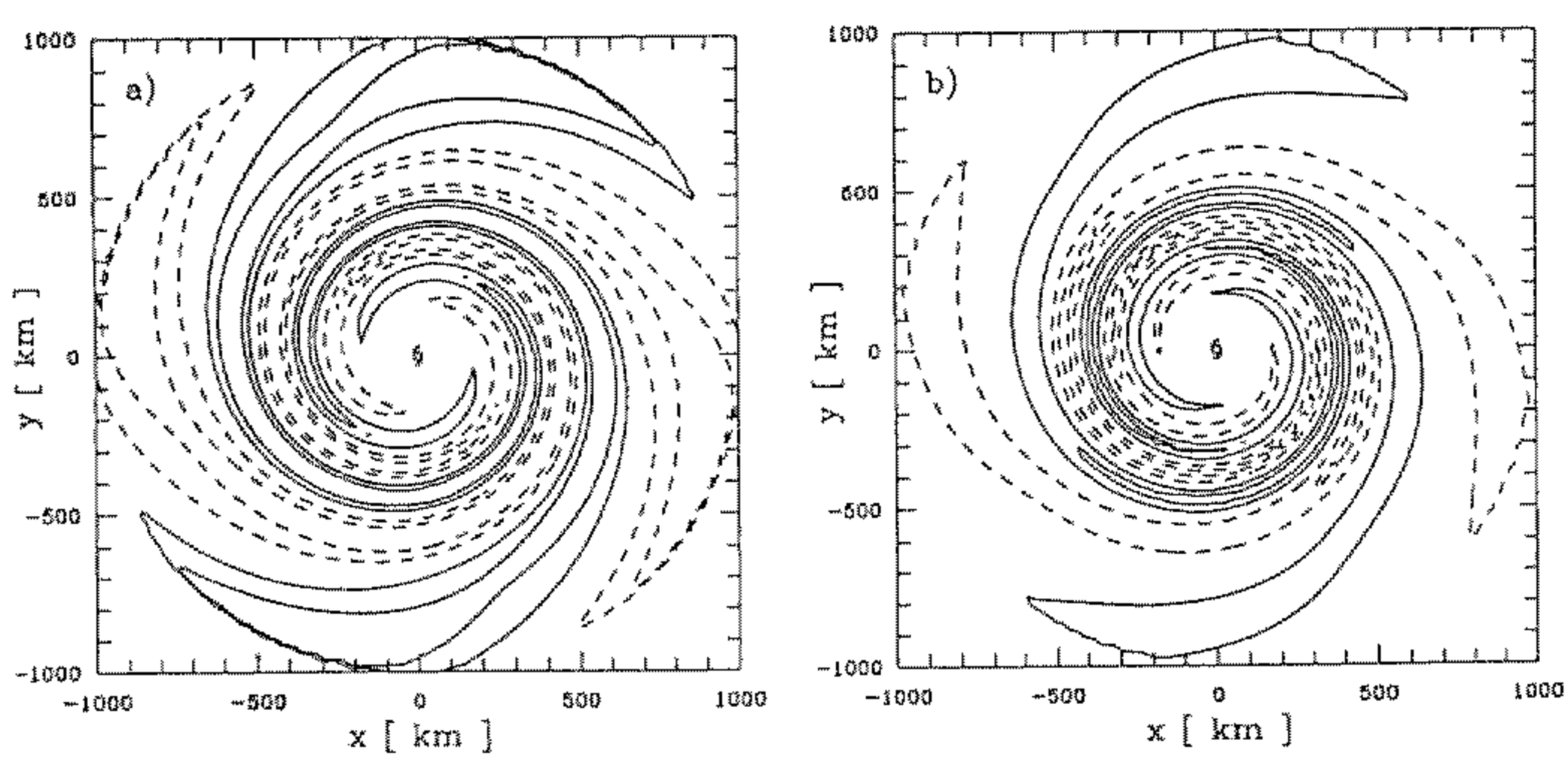

Figure 8. Wave-number 2 vorticity symmetry on (a) 11 October and (b) 12 October 1984, calculated on the assumption that the observed wave-number 2 asymmetry on the previous day is simply rotated and sheared by the mean tangential circulation during the period. The contour interval is 5.0×10^{-4} s^{-1} and dashed lines indicate negative values.

vorticity that is conserved following air parcels (Hoskins *et al.* 1985). By 'intrinsically baroclinic' we mean flows in which the structure of both the vortex and its environment vary with height. We consider a particular scenario in which relative-vorticity asymmetries in a baroclinic atmosphere may not suffer rotation and distortion by the tangential circulation of a vortex as described above, at least not to the same degree. If these asymmetries happen to be associated with PV anomalies concentrated solely at the tropopause, relative vorticity of one sign or another will be generated locally throughout the troposphere as air columns moving beneath the anomaly are stretched or shrunk as they seek to remain in

hydrostatic and gradient-wind balance (see, for example, Hoskins *et al.* (1985, p. 907)). Again the relative-vorticity asymmetries are locally forced, in this case by the divergent circulation rather than the horizontal deformation that forces ζ_{a2} in Eq. (3). However, where there is no perturbation potential vorticity, differential advection by the tangential shear has no effect on the PV distribution. In the absence of diabatic or frictional effects, the relative-vorticity anomalies that occur are accompanied by changes in static stability so as to keep the PV constant following air parcels. Accordingly, relative-vorticity anomalies associated with such upper-level PV anomalies will be tied to the upper anomaly. In the tropical-cyclone context, the evolution and motion of the upper anomaly will be governed by the flow fields near the tropopause which may have little to do directly with the vortical motion throughout most of the troposphere. However, it may be greatly influenced by the motion in the outflow layer of the storm which, typically, has an anticyclonic sense of rotation beyond a certain radius of the storm centre.

A way to determine the extent to which the asymmetries observed in Hurricane *Josephine* were associated with such anomalies would be to compare the pattern of PV asymmetry with that of relative vorticity. The former will be wound up by the tangential shear while the latter may not be. We have made an attempt to do this using the data available below 400 hPa in Hurricane *Josephine*.

Figure 9 compares the total 850–500 hPa layer-mean relative-vorticity asymmetry with the corresponding PV asymmetry. The latter was obtained as follows. First the temperature data from the ODWs were analysed using the Pedder objective-analysis scheme (HRD did not carry out an objective analysis of these data) and the pressure distribution, p, on selected isentropic surfaces ($\theta = 305$ K–325 K in steps of 5 K) was determined. The relative-vorticity data were then interpolated to these surfaces and the PV calculated using the formula $\mathrm{PV} = -g(f + \zeta)/(\partial\theta/\partial p)$. The background PV on each surface was obtained from the equation $\overline{\mathrm{PV}} = -gf/(\partial\bar{\theta}/\partial p)$, where an overbar denotes a zonal mean, and then the PV anomaly, defined as $\mathrm{PV}' = \mathrm{PV} - \overline{\mathrm{PV}}$, was calculated. This anomaly was averaged over the 305–325 K isentropic layer and the result divided by the volume mean of $-g\partial\bar{\theta}/\partial p$ to give the layer average of PV′ in units of vorticity. Finally, a symmetric mean of the anomaly was removed to give the fields shown in Fig. 9. While there are some differences in detail between the PV asymmetry and the relative-vorticity asymmetry, the larger-scale features are mostly similar, especially in the outer part of the vortex. The conclusion of this section is that the relative-vorticity anomalies in the 850–500 hPa layer-mean *are* associated with PV anomalies in that layer and therefore should be subject to rotation and filamentation by the symmetric circulation. They are not merely a result of PV anomalies concentrated above the 500 hPa level, for example, anomalies concentrated near the tropopause.

(g) *Vortex motion*

In the simple-barotropic-model calculations referred to in section 1, the wave-number 1 flow asymmetry across the vortex centre characterizes the drift of the vortex relative to the large-scale flow across its centre, i.e. the motion vector is closely approximated by the vector sum of the large-scale flow at the vortex centre, $\mathbf{U}_0$, and the flow at that point, $\mathbf{U}_a$, associated with the wave-number 1 component of the vorticity asymmetry—see, for example, Ulrich and Smith (1991) and Kraus *et al.* (1995). It is of interest, therefore, to examine whether these simple-model results are applicable to Hurricane *Josephine*. We consider two possible ways to estimate the asymmetric flow component across the vortex centre. The most direct method would appear to be to carry out an azimuthal analysis of one of the layer-mean velocity fields as outlined in appendix B. An alternative would be to invert the azimuthal wave-number 1 component of the layer-mean relative-vorticity

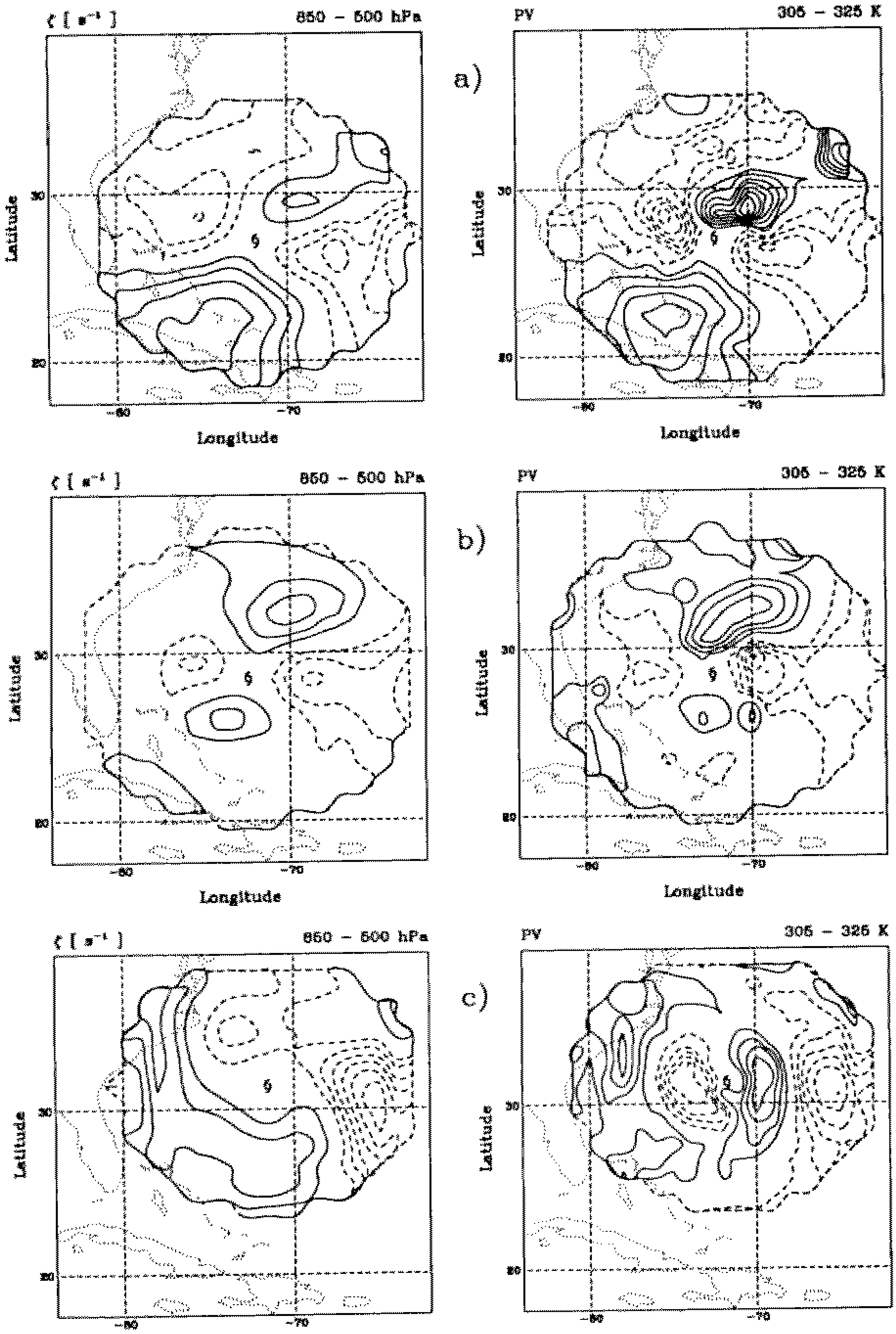

Figure 9. Total asymmetry of the relative vorticity averaged over the 850–500 hPa layer (left panels) compared with the potential-vorticity asymmetry (right panels) averaged over the layer between the 305 K and 325 K isentropic-surfaces (these two averaging layers approximately coincide) flow at the three analysis times: (a) 10 October, (b) 11 October, and (c) 12 October 1984. Contour interval is 2.5×10^{-4} s^{-1} and dashed lines indicate negative values; to facilitate a comparison of the different fields, the PV values have been converted to vorticity units as explained in the text.

field (i.e. to solve the Poisson equation $\nabla^2\Psi_a = \zeta_a$, subject to suitable boundary conditions on the stream function, Ψ_a, associated with this asymmetry). According to the above discussion, it would seem to be appropriate to subtract from these fields the large-scale environment, before carrying out the analysis, in order to compare the results with theory. However, we shall argue that this is unnecessary because, in the direct method, the flow at the vortex centre is simply the value at that point obtained from the original objective analysis (see appendix B). If the environmental value were removed, it would have to be added again after the analysis to obtain the total flow at the vortex centre.

Figure 10 shows the total wave-number 1 asymmetry for the 850–500 hPa layer-mean flow at the three analysis times, together with the corresponding asymmetries with the environmental flow removed. What is striking in these fields is that the flow near the vortex centre is relatively uniform, especially considering the paucity of ODW data near the vortex centre. This uniformity is presumably because of the inherent smoothing introduced at an earlier stage by the objective-analysis scheme. It is interesting to note also that the large-scale environment as we have defined it accounts for much of the asymmetric flow within a few hundred kilometres of the vortex centre, except in the immediate vicinity of the storm centre on 12 October.

With the above considerations, we would argue that, in as much as the barotropic theory of vortex motion is valid for either of the layer means obtained for Hurricane *Josephine*, the flow across the vortex centre in the wave-number 1 component of the total flow (Fig. 10, left panels) should characterize the steering flow for the storm. The extent to which this is the case is indicated in Table 5 which compares the magnitude and orientation of this flow component, $|\mathbf{U}_t|$ and φ_t, calculated for both the 850–500 hPa layer-mean and DLM flows with the observed translation speed and direction of the hurricane, $|\mathbf{U}_{obs}|$, and φ_{obs}. The calculated velocities are based on an average over a region within 200 km of the hurricane centre*. The agreement is not especially good for either layer mean and we can only conclude that, at least as far as the wave-number 1 asymmetries are concerned, the barotropic theory is either inapplicable or inaccurate in the case of Hurricane *Josephine*. The discrepancies between the observed storm speed and the value calculated gives a measure of the initial speed error which would arise in using a particular analysis to initialize a barotropic forecast model.

We have not pursued the alternative method for determining the asymmetric flow, partly because of the uncertainties in prescribing suitable boundary conditions on Ψ_a.

TABLE 5. SPEED $|\mathbf{U}_{obs}|$, AND DIRECTION φ_{obs}, OF THE STORM-MOTION VECTOR ON THE THREE OBSERVATION DAYS COMPARED WITH THE ESTIMATED CONTRIBUTIONS THERETO, $|\mathbf{U}_t|$ AND φ_t, FROM THE TOTAL ASYMMETRIC FLOW OF THE 850–500 hPa LAYER-MEAN FLOW AND THE DEEP-LAYER MEAN FLOW. THE ANGLES φ_{obs} AND φ_t ARE MEASURED CLOCKWISE FROM NORTH AND INDICATE THE DIRECTION FROM WHICH THE STORM/WIND MOVES/BLOWS.

Date	850–500 hPa	Deep-layer mean	Observed
10 October 1984	$\|\mathbf{U}_t\| = 3.1$	$\|\mathbf{U}_t\| = 2.5$	$\|\mathbf{U}_{obs}\| = 2.2$
	$\varphi_t = 123$	$\varphi_t = 135$	$\varphi_{obs} = 158$
11 October 1984	$\|\mathbf{U}_t\| = 1.3$	$\|\mathbf{U}_t\| = 2.9$	$\|\mathbf{U}_{obs}\| = 3.4$
	$\varphi_t = 186$	$\varphi_t = 142$	$\varphi_{obs} = 187$
12 October 1984	$\|\mathbf{U}_t\| = 3.4$	$\|\mathbf{U}_t\| = 4.5$	$\|\mathbf{U}_{obs}\| = 3.8$
	$\varphi_t = 157$	$\varphi_t = 196$	$\varphi_{obs} = 187$

* It turns out that there is little difference between the average value and the corresponding centre value in each case.

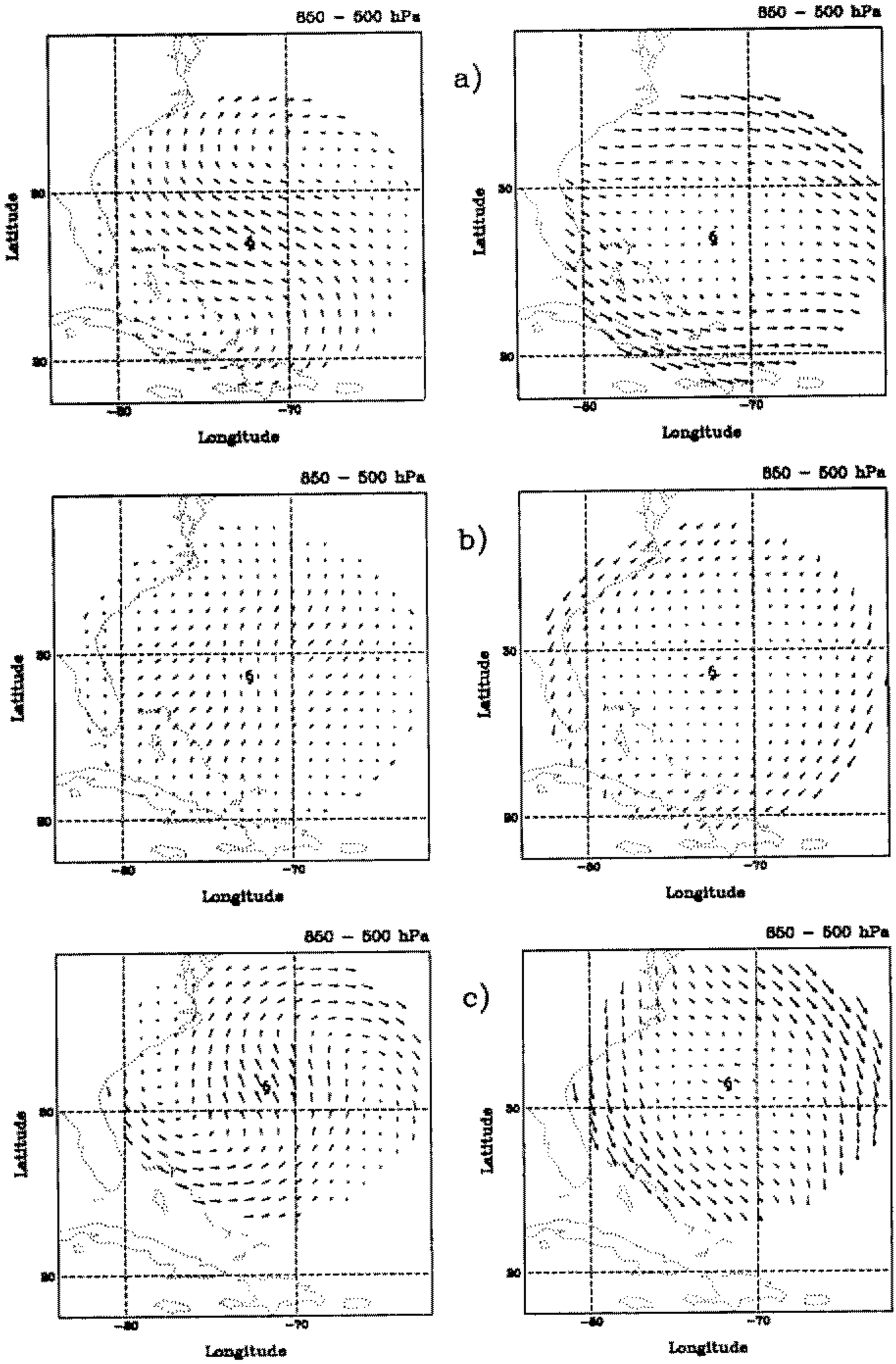

Figure 10. Total wave-number 1 asymmetry of the 850–500 hPa layer-mean wind field (left panels) at the three analysis times: (a) 10 October, (b) 11 October, and (c) 12 October 1984, together with the corresponding asymmetry with the environmental flow removed (right panels). A vector length of 2° latitude corresponds with a wind speed of 10 m s^{-1}.

Also, because the flow of either layer mean is not exactly nondivergent, one would need to introduce a velocity potential as well as the stream function to represent the total velocity. Nevertheless, in this case also, the removal of the environment before the azimuthal analysis would simply change the boundary conditions and, since the boundary-value problem is linear, the total asymmetric flow across the vortex centre would be the same as for an inversion of the total vorticity field (recall that the environment as defined in subsection (a) has uniform vorticity).

4. Discussion and conclusions

We have used one of the most comprehensive data sets so far obtained to study the structure and evolution of the outer circulation of an individual hurricane, i.e. the circulation beyond a radius of about 300 km from the centre. In particular we have sought to investigate the evolution of the asymmetries in both the 850–500 hPa layer-mean and the deep-layer mean vorticity fields and to determine the extent to which these asymmetries can be related to the layer-mean horizontal structure of the large-scale environment and to the storm motion on the basis of simple barotropic theories. The study complements that of Franklin (1990).

Hurricane *Josephine* intensified during three days over which the storm was monitored, but significant changes in the symmetric circulation were apparent only to about 500 km from the storm centre. At radii, larger than this, the circulation actually diminished slightly. At all radii, and on all three days, the decay of the mean tangential velocity was appreciably faster than the inverse of the radius, consistent with the relative vorticity being negative beyond a radius of between 400 and 450 km from the centre. The estimate for the vorticity of the large-scale environment obtained from the analysis described in section 3(c) is small and positive during the period of observation (see Table 2). Interestingly, the maximum value (6.0×10^{-8} s^{-1}) is much smaller than values at outer radii in the vorticity profiles in Fig. 1 which are on the order of 10^{-5} s^{-1}.

The structure and strength of the wave-number 1 vorticity asymmetries on 10 and 12 October 1984 are remarkably similar to those which occur in simple barotropic models, but the major change in orientation and strength of the observed asymmetry over the three-day period is difficult to interpret in the light of barotropic theory. This change might be a result of the vertical shear of the storm environment.

The wave-number 2 asymmetry is a prominent feature of the total vortex asymmetry on 10 October 1984, but it weakened during the period of observation, a feature noted by Franklin (1990, p. 2741). Its orientation varied little during this period and is consistent with it being related to that of the large-scale deformation field. Moreover, the strength of this asymmetry is a monotonic function of that of the deformation field as theory would indicate.

It is difficult to draw firm conclusions from this single case study, and more analyses of data from individual storms are clearly called for. Nevertheless, our analysis provides a framework for further studies when suitable data sets become available. Indeed, it demonstrates the need to obtain multiple realizations of the storm structure to enable the evolution of the vortex asymmetries to be investigated.

Of course, one must recognize that baroclinic effects may be particularly important in some cases and we should point out that Hurricane *Josephine* was notable for the baroclinic nature of its environment (Franklin 1990, p. 2740). At the present time, the baroclinic theory of tropical-cyclone motion is less well advanced than the barotropic

theory, and a comprehensive investigation of baroclinic effects is beyond the scope of this paper.

The study highlights the urgent need to obtain wind and temperature data in the upper troposphere with a resolution adequate to determine the potential-vorticity distribution in that region, a requirement that presents a challenge to the development of new measurement platforms.

Acknowledgements

We would like to express our sincere thanks to James Franklin and Lloyd Shapiro at the Hurricane Research Division and Noel Davidson of the Australian Bureau of Meteorology Research Centre for their perceptive comments on earlier versions of the manuscript, to James Franklin for providing the data, to Mike Pedder at the University of Reading for his advice on matters concerning objective analysis and for allowing us to use a computer algorithm that he had developed, and to Dan Keyser at the State University of New York at Albany for discussions relating to section 3(f). Finally we acknowledge financial support from the US Office of Naval Research through Contract Nos N00014-90-J-1487 and N00014-95-1-0394.

Appendix A

More on the large-scale environment

Let (U_r^*, U_θ^*) denote the large-scale environmental flow defined in subsection 3(a) and (U_r, U_θ) the observed wind field, respectively, expressed in polar coordinates centred on the vortex. It follows readily that

$$\left.\begin{aligned} U_r^* &= U_{r0} + \tfrac{1}{2} r D_0 + \tfrac{1}{2} r (E_0 \cos 2\theta + F_0 \sin 2\theta) \\ U_\theta^* &= U_{\theta 0} + \tfrac{1}{2} r \zeta_0 + \tfrac{1}{2} r (E_0 \sin 2\theta - F_0 \cos 2\theta) \end{aligned}\right\} \tag{A.1}$$

where $U_{r0} = U_0 \cos\theta + V_0 \sin\theta$, and $U_{\theta 0} = -U_0 \sin\theta + V_0 \cos\theta$. Let $\langle\ \rangle$ denote the average over a cylindrical domain of radius R, i.e. $\langle\phi\rangle = (1/\pi R^2) \int_0^{2\pi} \mathrm{d}\theta \int_0^R \phi r \, \mathrm{d}r$ and define

$$\Delta = \langle (U_r - U_r^*)^2 + (U_\theta - U_\theta^*)^2 \rangle.$$

The best fit of (A.1) to the data is obtained when $\partial\Delta/\partial\lambda = 0$, where λ denotes any one of the constants U_{r0}, $U_{r\theta}$, D_0, ζ_0, E_0, F_0. It follows readily from the six equations obtained in this way that

$$U_{r0} = \langle U_r \rangle, \qquad U_{\theta 0} = \langle U_\theta \rangle$$

$$D_0 = (4/R^2)\langle r U_r \rangle, \qquad \zeta_0 = (4/R^2)\langle r U_\theta \rangle$$

$$E_0 = (4/R^2)\langle r (U_r \cos 2\theta - U_\theta \sin 2\theta) \rangle, \; F_0 = (4/R^2)\langle r (U_r \sin 2\theta - U_\theta \cos 2\theta) \rangle.$$

The first two of these relations show that the large-scale flow at the vortex centre is just the mean of the total flow in a circular region surrounding this centre. The large-scale vorticity and divergence contribute symmetric components to U_{r0}, and $U_{\theta 0}$, and therefore azimuthal wave-number 1 components to the Cartesian velocity components, U^* and V^*. The large-scale deformation field characterized by the terms involving E_0 and F_0 corresponds with a wave-number 1 asymmetry of U^* and V^* also, but it appears as a wave-number 2 component of U_r, and U_θ. Because it is irrotational, it does not project onto the flow components associated with the wave-number 2 vorticity asymmetries described in subsections 3(c) and (d).

Appendix B

Azimuthal analysis of the total wind field

The radial and tangential wind components, U_r, and U_θ, can be represented by Fourier series with the form:

$$U_r(r, \theta) = a_0 + \sum_{n=1}^{\infty}(a_n(r) \cos n\theta + b_n(r) \sin n\theta)$$
$$U_\theta(r, \theta) = c_0 + \sum_{n=1}^{\infty}(c_n(r) \cos n\theta + \mathrm{d}_n(r) \sin n\theta)$$

where a_0 and c_0 are constants equal to the centre values of U_r and U_θ, respectively, and for $n \geqslant 1$,

$$(a_n, c_n) = 2\int_0^{2\pi} (U_r, U_\theta) \cos n\theta \, \mathrm{d}\theta$$

and

$$(b_n, d_n) = 2\int_0^{2\pi} (U_r, U_\theta) \sin n\theta \, \mathrm{d}\theta.$$

This analysis described in subsection 3(g) was carried out using a standard fast-Fourier transform package after the velocity data had been interpolated on to a suitable system of polar coordinates centred on the vortex centre.

References

Davies-Jones, R. P. 1993 Useful formulae for computing divergence, vorticity, and their errors from three or more stations. *Mon. Weather Rev.*, **121,** 713–725

Fiorino, M. and Elsberry, R. L. 1989 Some aspects of vortex structure related to tropical cyclone motion. *J. Atmos. Sci.*, **46,** 975–990

Franklin, J. L. 1990 Dropwindsonde observations of the environmental flow of Hurricane Josephine (1984): Relationships to vortex motion. *Mon. Weather Rev.*, **118,** 2732–2744

Hoskins, B. J., McIntyre, M. E. and Robertson, A. W. 1985 On the use and significance of isentropic potential vorticity maps. *Q. J. R. Meteorol. Soc.*, **111,** 877–946

Jones, S. C. 1995 The evolution of vortices in vertical shear. I: Initially barotropic vortices. *Q. J. R. Meteorol. Soc.*, **121,** 821–851

Kasahara, A. and Platzmann, G. W. 1963 Interaction of a hurricane with a steering field and its effect upon the hurricane trajectory. *Tellus*, **15,** 321–335

Kraus, A. B., Smith, R. K. and Ulrich, W. 1995 The barotropic dynamics of tropical cyclone motion in a large-scale deformation field. *Contrib. to Atmos. Phys.*, **68,** 249–261

Pedder, M. A. 1993 Interpolation and filtering of spatial observations using successive corrections and Gaussian filters. *Mon. Weather Rev.*, **121,** 2889–2902

Reeder, M. J., Smith, R. K. and Lord, S. H. 1991 The detection of flow asymmetries in the tropical cyclone environment. *Mon. Weather Rev.*, **119,** 848–854

1992 Reply to comments by Holland *et al. Mon. Weather Rev.*, **120,** 2398–2400

Shapiro, L. J. and Ooyama, K. V. 1990 Barotropic vortex evolution on a beta plane. *J. Atmos. Sci.*, **47,** 170–187

Smith, R. K. 1991 An analytic theory of tropical-cyclone motion in a barotropic shear flow. *Q. J. R. Meteorol. Soc.*, **117,** 685–714

Smith, R. K. and Ulrich, W. 1990 An analytic theory of tropical-cyclone motion using a barotropic model. *J. Atmos. Sci.*, **47,** 1973–1986

1993 Vortex motion in relation to the absolute vorticity gradient of the vortex environment. *Q. J. R. Meteorol. Soc.*, **119,** 207–215

Smith, R. K. and Weber, H. C. 1993 An extended analytical theory of tropical-cyclone motion in a barotropic shear flow. *Q. J. R. Meteorol. Soc.*, **119,** 1149–1166

Smith, R. K., Ulrich, W. and Dietachmayer, G. 1990 A numerical study of tropical-cyclone motion using a barotropic model. I: The role of vortex asymmetries. *Q. J. R. Meteorol. Soc.*, **116,** 337–362

Ulrich, W. and Smith, R. K. 1991 A numerical study of tropical-cyclone motion using a barotropic model. II: Motion in spatially-varying large-scale flows. *Q. J. R. Meteorol. Soc.*, **117**, 107–124

Weber, H. C. and Smith, R. K. 1995 Data sparsity and the tropical-cyclone analysis and prediction problem: Some simulation experiments with a barotropic numerical model. *Q. J. R. Meteorol. Soc.*, **121**, 631–654